IECMS 2020

sciforum

Conference Proceedings Paper

Microthermometry Considerations Basiran (SW Birjand) and Kanif (SE Birjand) Manganese Prospects, Birjand, South-Khorasan, East of Iran

Behnaz Barghi [1], Ahmad Azargoon Jahromi [2]*

[1] Geology Department, University of Birjand, Birjand, Iran; barghibehnaz@yahoo.com
[2] Department of Mining and Metallurgical Engineering Yazd University, Yazd, Iran; ahmad.azargoon@gmail.com
* Correspondence: ahmad.azargoon@gmail.com; Tel: +98-991-380-1400

Received: date; Accepted: date; Published: date

Abstract: The studied manganese prospects (1) Kanif is in ophiolitic complex are located in 110 km southeast of Birjand, Southern Khorasan province (east of Iran). The ophiolitic sequence in this region hosts manganese ore occurring as small discrete patche associated with radiolarian cherts. Ore minerals identified by XRD method and petrographic studies are pyrolusite, hematite, and goethite showing replacement, colloidal and brecciated textures. Carbonate and silica are the gangue minerals. Based on the ICP-ES-MS methods, the average grade of Mn in Kanif is 33.92%. Microthermometry considerations of calcite in Kanif, fluid inclusions demonstrated that the ore-forming solutions had salinities within the range of 0.5-4.5 wt% NaCl eq., homogenization temperature range of 100-220˚C and density about 0.8-1 g/cm3. The pressure was estimated to be about 50 bars which corresponds with a depth of ~150 meters at the time of formation ophiolite-hosted manganese prospects.(2) Basiran veins/veinlets are located in 212 km southwest of Birjand, Southern Khorasan province (east of Iran). These veins/veinlets are hosted by andesitic rocks of Eocene to Oligocene ages. Ore minerals identified by XRD method and petrographic studies are pyrolusite, psilomelane, hematite, goethite and limonite, displaying colloform and open-space filling textures. Gypsum, carbonate and silica are the gangue minerals. Alteration zones, specifically argillic alteration zone, are developed along the veins/veinlets within the andesitic wall rocks. Based on the mineralogical and geochemical data, the primary manganese minerals were Mn oxides and hydroxides, which have gradually been converted to psilomelane and finally pyrolusite. The average grade of Mn within the veins/veinlets are 25.95%. Microthermometry considerations of calcite in Kanif, fluid inclusions demonstrated that the ore-forming solutions had salinities within the range of 0.5-5.5 wt% NaCl eq., TH range of 120-220˚C and density about 0.8-1 g/cm3. The pressure was estimated to be less 50 bars which corresponds with a depth of ~150 meters that in this area show hydrothermal origin. The Major purpose this study are investigation fluid inclusions based on petrography, Variety, morphologies, salinity, Homogenization temperature for polykind of the manganese prospects in different locations: Kanif is located in sistan zone and Basiran is located in lut block that Results and Interpretation of microthermometric data suggested a hydrothermal origin for the Kanif and Basiran Mn prospects.

Keywords: Mn prospects; Kanif, Basiran; Andesite, Pyrolusite; Psilomelane; Microthermometry; Fluid inclusions.

1. Introduction

Fluids inclusions small volumes of fluid in a crystal that may be lost along the growth zones or inside the cavities of any crystal lattice defect during crystal growth[1]. The study of fluids inclusions in manganese deposits is an important aid in the diagnosis of physical and chemical conditions hydrothermal fluids responsible for the development and evolution of mineralization and alteration processes. The study of fluids inclusions in gangue minerals (quartz and calcite) in manganese veins in alteration and ore-forming zones in the manganese remain in Basiran prospect (south-west) and Kanif prospect (south-east) Birjand (figure 1).

2. Method of investigation

Fluid inclusions studies have been performed mainly on manganese ore samples containing quartz and carbonate veins. In this regard, 12 samples were selected and doubly-polished sections were prepared (2 samples of calcite veins in Basiran prospect and 2 samples of calcite veins in Kanif prospect). After petrographic and mineralogical studies, 4 of these sections were analyzed by microthermometry (2 samples of calcite veins in Basiran prospect, and 2 samples of calcite veins in Kanif prospect). Microthermometric studies of fluids inclusions with Zeiss microscope Linkam stage, Model THMS600 And with a magnifying lens of 800 and 1250 magnification at the Minerals Laboratory of the Iranian Minerals Processing Research Center located in Karaj. The temperature range is -196 to +600 degrees Celsius. It also comes with two controllers: heating (TP94) and cooling (LNP), an azotic tank (for nitrogen pumps for freezing) and a water tank (for cooling the device at high temperatures). The following standards were used to calibrate the device:
Calibration with Tolerance:
Heating: ±0.6, Freezing: ±0.2
Heating: Sodium nitrate, melting point: +308ºC
Freezing: n-Hexane, melting point: -94.3ºC
Fluid inclusions petrographic studies have also been carried out at magnifications of 500, 800, 625, and 1250 at the Mineral Processing Research Center.

3. Discussion

In the petrographic study, the types of primary, secondary, and pseudo-secondary inclusions involved were identified in the studied samples (figure 2 and 3). Proximity and Solidification between Manganese Oxide Minerals and Calcite Crystals and the quartz in the veinlets indicates that they are cohesive and have the same source of fluid production. The information obtained from these studies can also be generalized to the conditions for the formation of manganese oxides and consequently the ore deposit.

3.1. Fluid inclusions petrography

In the petrographic study, the types of primary, secondary, and pseudo-secondary inclusions involved were identified in the studied samples (figure 2 and 3). Proximity and Solidification between Manganese Oxide Minerals and Calcite Crystals and the quartz in the veinlets indicates that they are cohesive and have the same source of fluid production. The information obtained from

these studies can also be generalized to the conditions for the formation of manganese oxides and consequently the ore deposit

3.2. Variety of fluid inclusions

In total, 1 main fluid-type has been identified in the studied samples, including two-phase fluid (liquid-vapor) fluid-rich fluid. As noted at the outset, the selected samples for these studies are mainly quartz veins and carbonate veinlets. Carbonate veinlets contain manganese oxide minerals. The thickness of the carbonate veinlets collected is about 5 mm in the hand sample. In these veins the carbonate (calcite) is fine to medium and manganese oxides in the space between the rhomboid crystals and calcite mosaic are seen, the dimensions of the fluids involved in carbonates are between 1 and 30 microns. In the quartz veinlets, the dimensions of the fluids involved were less than 4 microns, and therefore microthermometric analysis was not performed on them.

3.3. Fluid inclusions morphologies

The fluid inclusions forms involved are highly diverse and are partially controlled by host mineralogy crystallography. The fluids inclusions may take the negative crystalline form of the host minerals (eg, cubic in halite) or they may be highly irregular and broad. In fine minerals with fine cleavage, such as the rhombohedral carbonates, the fluid walls inclusions often develop along the host mineral surfaces. Spherical or turn-shaped are also common, especially in quartz, whereas tubular and flat fluid inclusions develop mainly in elongated and prismatic minerals such as apatite[2].

The primary fluids inclusions in the samples under study were relatively large (5–20 µm but most up to 15 µm) in Basiran prospect, and their distribution mainly linear along the calcite cleavage (figure 2, a) in rod shapes and the elongated ellipses (figure 2, b) are rectangular in shape and rods (Figures f, e, d, c,). Secondary and pseudo-secondary types are also found in the trail at the site of repaired calcite crystal fractures, which usually have smaller dimensions (1-5 microns) (figure 2, f). Rhombic shapes are also common in that the fluids inclusions in the negative crystalline form of calcite (Romboeder) (figure 2, g, h). Therefore, The primary fluids inclusions in the samples under study were relatively large (5–20 µm but most up to 15 µm) in Kanif prospect, the most important fluid inclusions forms observed in elongated, elliptical, and rectangular cones (figure 3, a, b). The negative shapes are crystalline, rhombic and have random spatial distribution without orientation. The narrowing phenomenon is visible in the samples studied (figure 3, c, d). The fluids inclusions in the secondary and pseudo-secondary inclusions in the samples studied are mostly to rows, boundary-to-boundary, boundary-to-grain, and intra-grain (figure 3, g, h).

Microthermometric studies were performed on 26 fluids inclusions in Basiran and 88 fluids inclusions in Kanif (Micrometric results are listed in Tables 9 and 10 in the Appendix).

3.4. Measuring salinity

The determination of salinity is carried out by the freezing process of the fluid inclusions. The findings obtained during the solidification process involve fluid composition and density. An inherent problem with freezing fluid inclusions is their resistance to freezing, which in turn requires cooling to very low temperatures. The temperature at which the fluid is frozen does not provide a reliable estimate of its composition, and the cooling rate for freezing is mostly determined by the presence or absence of crystalline nucleation sites. The irregularly shaped fluid inclusions have many nesting angles, and the fluid inclusions containing fine-grained solids contain good nucleation sites and, therefore, freeze near their actual freezing temperatures. But fluid inclusions with good rotation or those without solid particles require super-cooling. H2O-salt systems: Freezing studies are the best and most commonly used method for measuring salinity of hydrogen-encapsulated fluids, since the reduction of the freezing point of pure water is directly proportional to the amount of salt present in the solution. The salinity of the fluid inclusions is obtained by measuring the ultimate melting point (TM) during heating of the frozen fluid inclusions. Of course, TM varies depending on the nature of the salt present, and since the fluid composition is hardly determinable, they express the ice melting temperatures conventionally in terms of weight percent NaCl. In studying the salt-water systems, two further phases should be considered: the first appearance of the liquid after complete freezing and thawing of the salt hydrates. The first, known as the first TFM melting temperature, corresponds to the eutectic temperature. The eutectic temperature varies for the various compounds present in the fluid inclusions retardant[2]. The results of the salinity values obtained by the freezing process are listed in Tables 9 and 10 in the Appendix. The range of salinity changes obtained for Basiran and Kanif intermediates are 0.5-5 and 0.5 - 0.5 wt%, respectively (figure 4).

3.5. Homogenization temperature

The homogenization latent temperature in the fluid inclusions is determined by the Heating process. At homogenization temperature, the fluid is converted to a single-phase system. This temperature in usual condition, is total homogenization temperature (liquid-vapor) (TL-V) But for fluid inclusions containing daughter minerals, it can also be the solute phase dissolution temperature (TS). The final homogenization temperature (TS or TH), together with the findings from the solidification process, can be used to calculate the total fluid density. And rich liquid phase, showed a homogeneous temperature range of 120-220 °C at Basiran and 100-300 °C at Kanif (Figure 5).

4. Results and Interpretation of microthermometric data

In the fluidic salinity diagram versus TH (L-V) (figure 6), the two-phase fluid inclusions entrainment is below the halite saturation curve, indicating the undersaturated of the NaCl fluids. Also, according to this diagram, the fluid vapor pressure was mainly less than 50 times when the two-phase fluids trapped. The trend of the findings plotted in (Figure 6) shows a relatively narrow range of TH (L-V) and a narrow salinity interval. The salinity abundance in Basiran manganese prospect is 2.5-3 and the manganese prospect of Kanif is 1.5 to 2.5 percent by weight of NaCl and the homogenization temperature of the fluids involved is in the Basiran manganese prospect of 140-160 °C and in the Kanif prospect of 120-140 °C. The homogeneity of the fluid involved together with the salinity findings, regardless of the trapping conditions, determine the fluid density. Fluid density variations are important in that they control the flow mechanisms and fluid spatial variations in a system. The density is obtained by the use of common diagrams of homogeneity-salinity temperatures (figure 7), which are contoured by lines of constant values of fluid density. The findings of the fluids inclusions can be plotted on such diagrams and examined for density variations that for fluid-rich two-phase inclusions in Basiran, density of 0.9-1 g/cm3 and in two-phase rich fluid inclusions in Kanif this range is between 0.8-1 g/cm3.

Acknowledgement:

The authors would like to acknowledge the financial support provided by Research Deputy Bureau of the University of Birjand and Tabriz, and the experimental support by Iran Mineral Processing Research Center (Karaj). Our appreciation is further expressed to anonymous reviewers for making critical comments and suggestions on this manuscript.

Funding: "This research received no external funding"

Appendix A

Figure captions:

Fig. 1 Simplified structural map of Iran, and the location of volcanic rocks of east Iran and the study area in the Lut block[3].

Fig. 2 Photomicrographs of various shapes of fluids inclusions within calcite crystals present in manganese ore in Basiran, (a) Distribution of two-phase (L-V) shortcuts linearly along the calcite cleavages, (b) Indicator Mostly two-phase rods and elliptical shortcuts (L-V) (c, d, e, f) Biphasic rectangular inclusions (L-V), (f Trails of secondary and pseudo-secondary inclusions along microfracture surfaces (L-V), Are observed at the fractured site of calcite crystals, (g), (h) Sliding inclusions that have a negative crystalline form of the rhomboid calcite, and are often two-phase (L-V).

Fig. 3 Photomicrographs of various shapes of fluids inclusions within calcite crystals present in manganese ore in Kanif (a, b), showing rectangular, two-phase, elliptical (L-V) (c), (d) two-phase inclusions (L-V) that have a negative crystalline form of the rhomboid calcite, Rhombic, and have random spatial distribution without orientation, the narrowing phenomenon is visible in inclusions, (e) Rhombic inclusions (e, f) False secondary and secondary types are traced at the site of repaired calcite crystals; (g),(h) pseudo-secondary and secondary fluids involved in the samples studied, mostly in the row, Border to border, The boundaries are within the grain and within the grain.

Fig. 4 (a) Histogram showing the measured salinity of the liquid-rich 2-phase inclusions in calcite crystal at Basiran.(b) Histogram showing the measured solubility of the liquid-rich 2-phase inclusions in calcite crystal at Kanif.

Fig. 5 (a) Histogram showing the measured homogenization temperature (TH) of the liquid-rich 2-phase inclusions in calcite crystal at Basiran.(b) Histogram showing the measured homogenization temperature (TH) of the liquid-rich 2-phase inclusions in calcite crystal at Kanif.

Fig. 6 (a) Bivariate plot of TH(L-V) versus salinity at Basiran and (b) Bivariate plot of TH(L-V) versus salinity at Kanif, Shown on this figure are also the halite saturation curve, critical curve[4], and the dashed lines representing the homogenization pressures of the fluid inclusions at the indicated temperature and salinity[5,6]. Fig. 7 U-Th binary diagram and the location of the Jonub-e-Sehchangi data points within the hydrothermal field[7].

Fig. 7 (a) plot of TH(L–V) versus salinity (expressed as wt% NaCl eq.) at Basiran. (b) plot of TH(L–V) versus salinity (expressed as wt% NaCl eq.) at Kanif. showing densities (in g/cm3) of the studied liquid-rich 2-phase fluid inclusions[1]. Contours regressed from data generated by the equation-of-state[8].

Table 1 Microthermometric data obtained from fluid inclusions within calcite crystals in the Mn ores at Basiran.

Table 2 Microthermometric data obtained from fluid inclusions within calcite crystals in the Mn ores at Basiran.

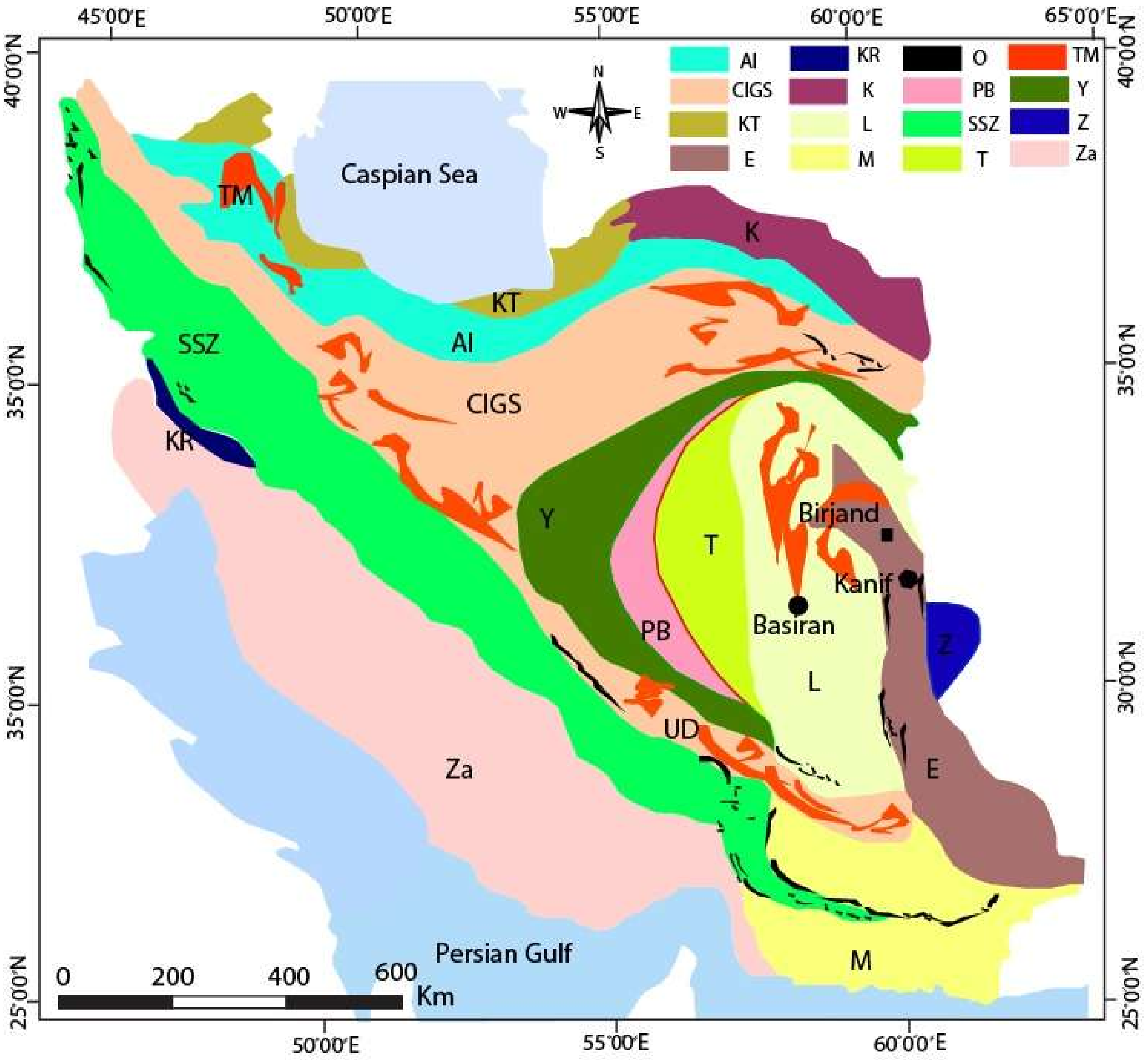

Al: Alborz ranges, CIGS:Central Iranian geological and structural gradual zone, E: East Iran ranges, K: Kopehdagh, KR:Kermanshah Radiolarites subzone, KT: Khazar-Talesh-Ziveh structural zone, L: Lut Block, M: Makran zone, O: ophiolite belts, PB: Posht-e-BadamBlock, SSZ: Sanandaj-Sirjan zone, T: Tabas Block, TM:tertiary magmatic rocks, UD: Urumieh-Dokhtar magmatic arc, Y:Yazd Block, Z : Zabol area, Za: Zagros ranges (● Mn- Basiran ⬢ Mn- Kanif).

Fig. 1 Simplified structural map of Iran, and the location of volcanic rocks of east Iran and the study area in the Lut block[3].

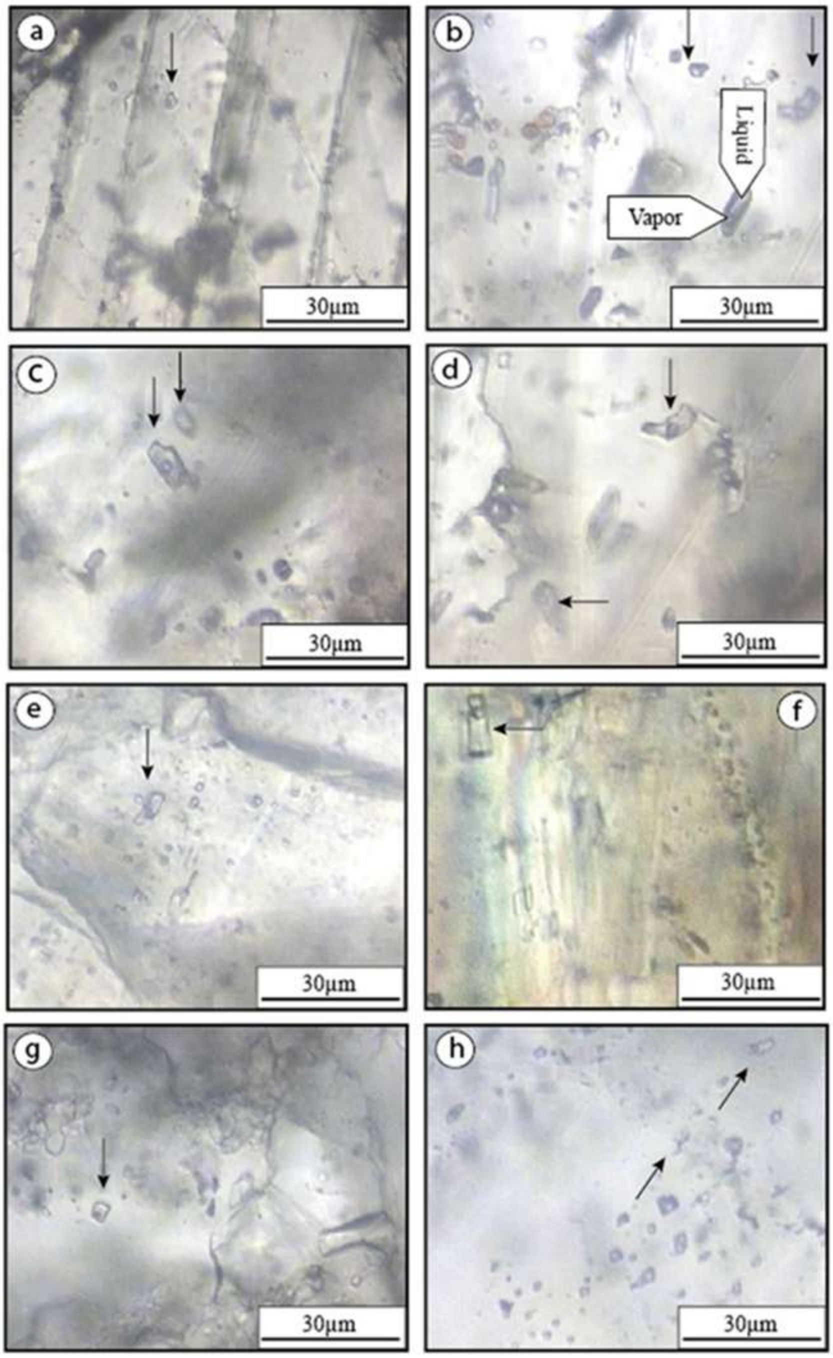

Fig. 2 Photomicrographs of various shapes of fluids inclusions within calcite crystals present in manganese ore in Basiran, (a) Distribution of two-phase (L-V) shortcuts linearly along the calcite cleavages, (b) Indicator Mostly two-phase rods and elliptical shortcuts (L-V) (c, d, e, f) Biphasic rectangular inclusions (L-V), (f Trails of secondary and pseudo-secondary inclusions along microfracture surfaces (L-V), Are observed at the fractured site of calcite crystals, (g), (h) Sliding inclusions that have a negative crystalline form of the rhomboid calcite, and are often two-phase (L-V).

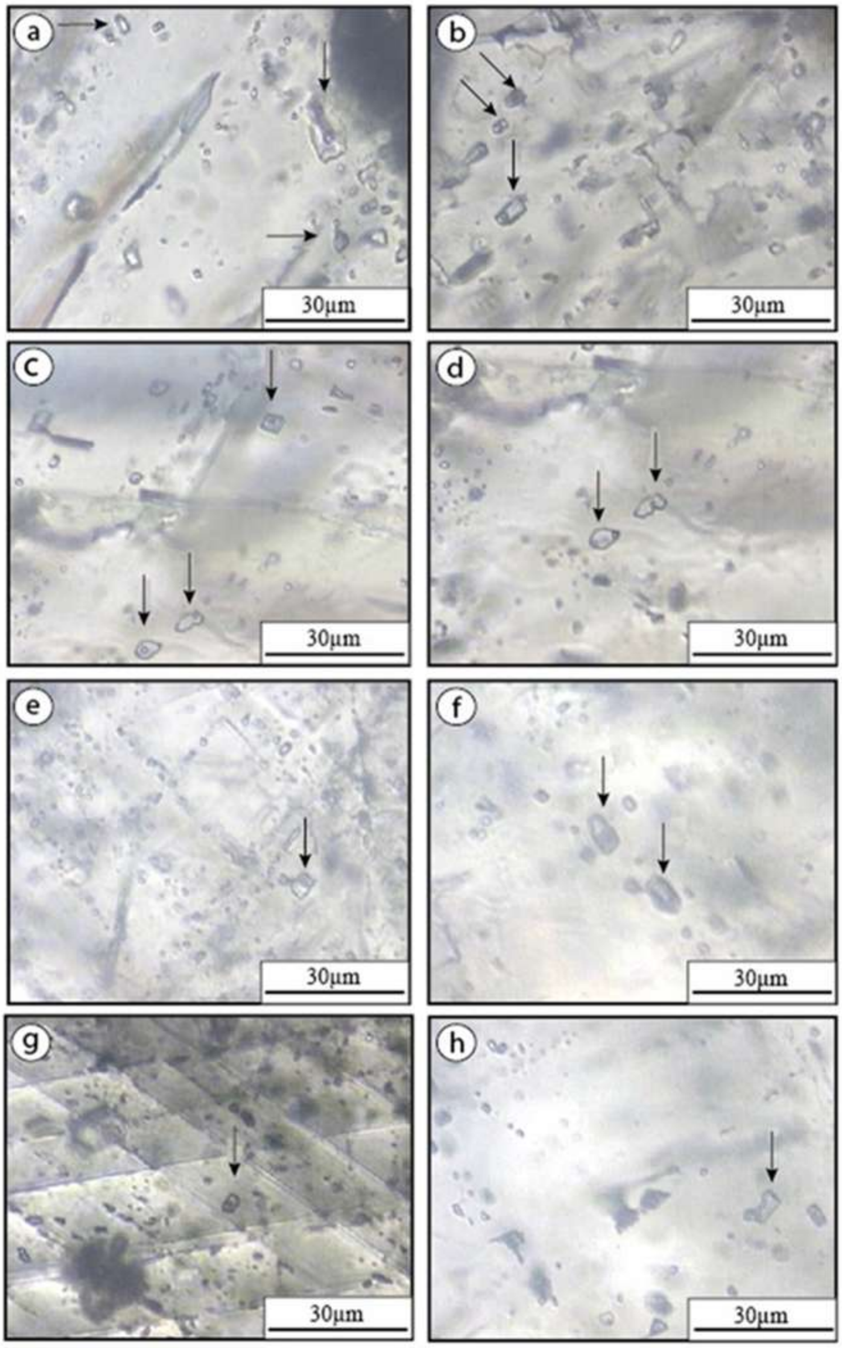

Fig.3 Photomicrographs of various shapes of fluids inclusions within calcite crystals present in manganese ore in Kanif (a, b), showing rectangular, two-phase, elliptical (L-V) (c), (d) two-phase inclusions (L-V) that have a negative crystalline form of the rhomboid calcite, Rhombic, and have random spatial distribution without orientation, the narrowing phenomenon is visible in inclusions, (e) Rhombic inclusions (e, f) False secondary and secondary types are traced at the site of repaired calcite crystals; (g),(h) pseudo-secondary and secondary fluids involved in the samples studied, mostly in the row, Border to border, The boundaries are within the grain and within the grain.

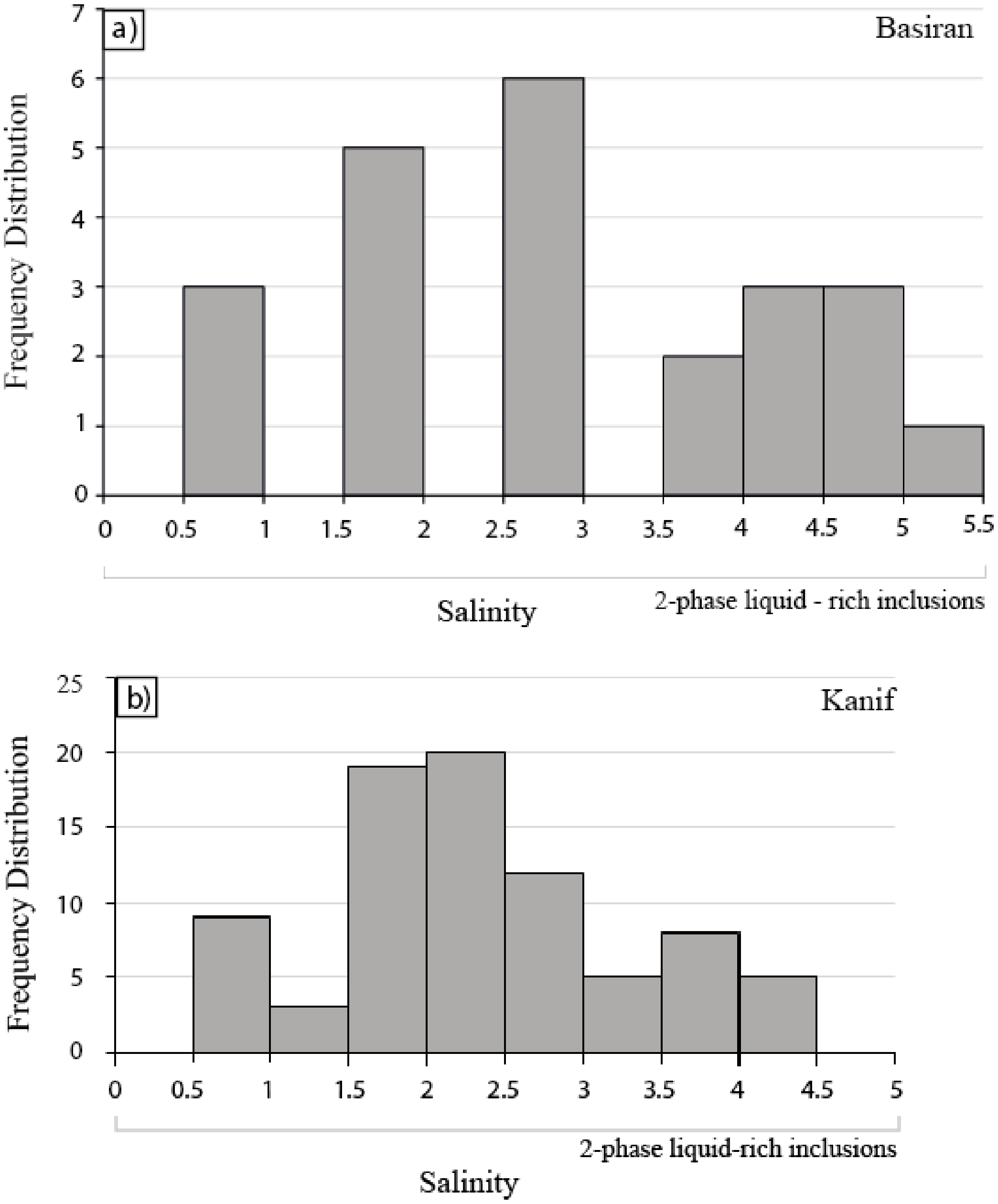

Fig.4 (a) Histogram showing the measured salinity of the liquid-rich 2-phase inclusions in calcite crystal at Basiran.(b) Histogram showing the measured solubility of the liquid-rich 2-phase inclusions in calcite crystal at Kanif.

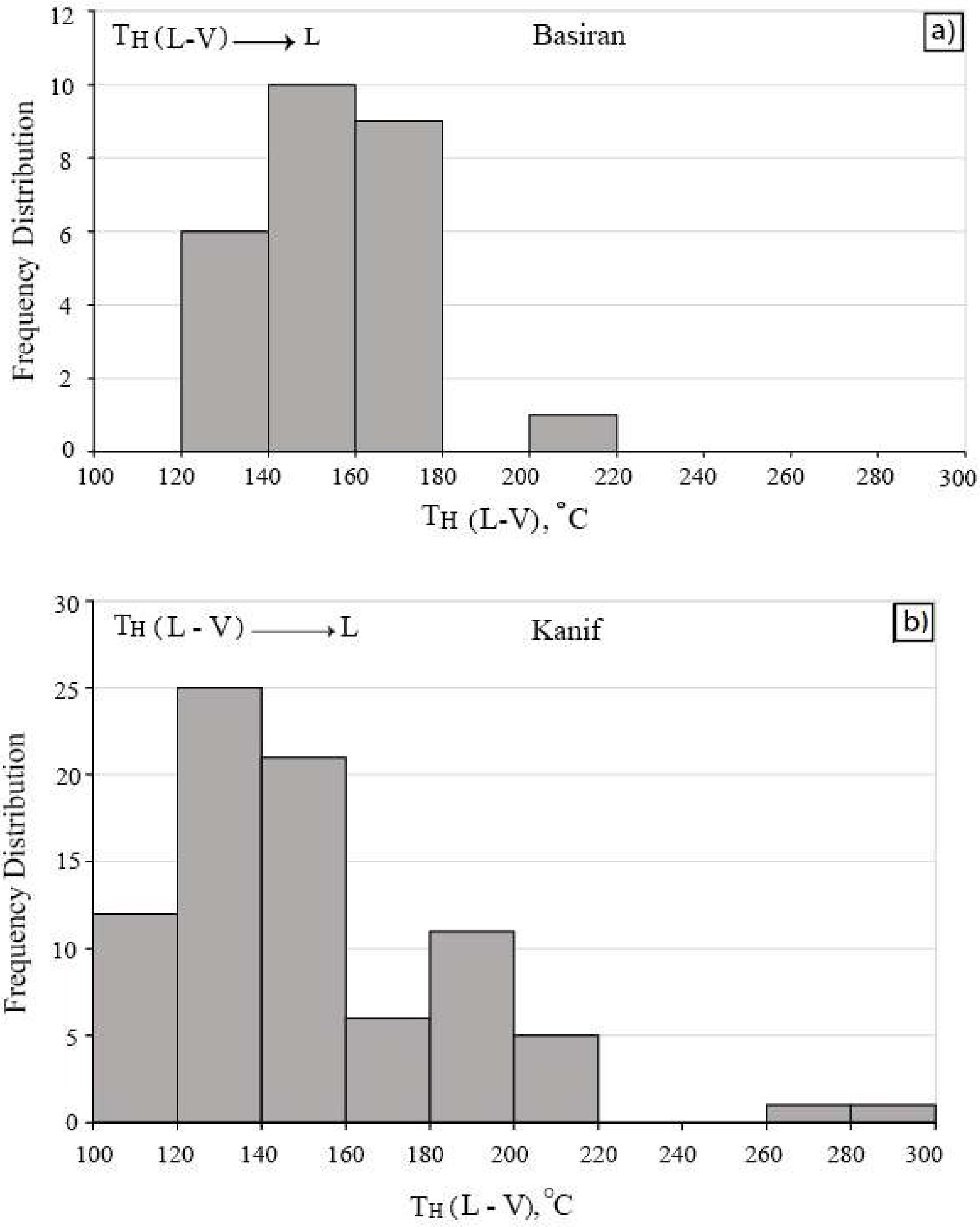

Fig.5 (a) Histogram showing the measured homogenization temperature (TH) of the liquid-rich 2-phase inclusions in calcite crystal at Basiran.(b) Histogram showing the measured homogenization temperature (TH) of the liquid-rich 2-phase inclusions in calcite crystal at Kanif.

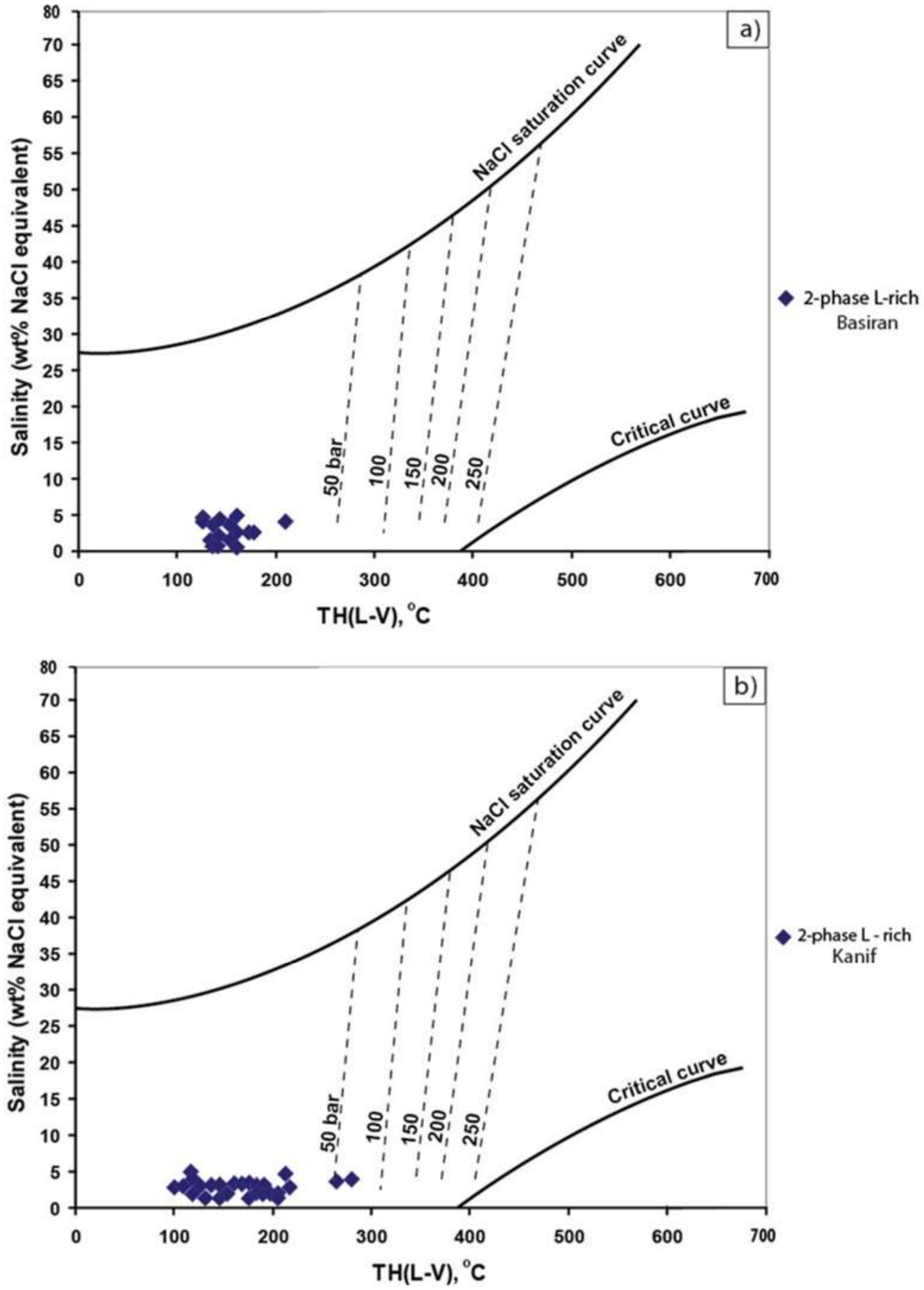

Fig.6 (a) Bivariate plot of TH(L-V) versus salinity at Basiran and (b) Bivariate plot of TH(L-V) versus salinity at Kanif, Shown on this figure are also the halite saturation curve, critical curve[4], and the dashed lines representing the homogenization pressures of the fluid inclusions at the indicated temperature and salinity[5,6].

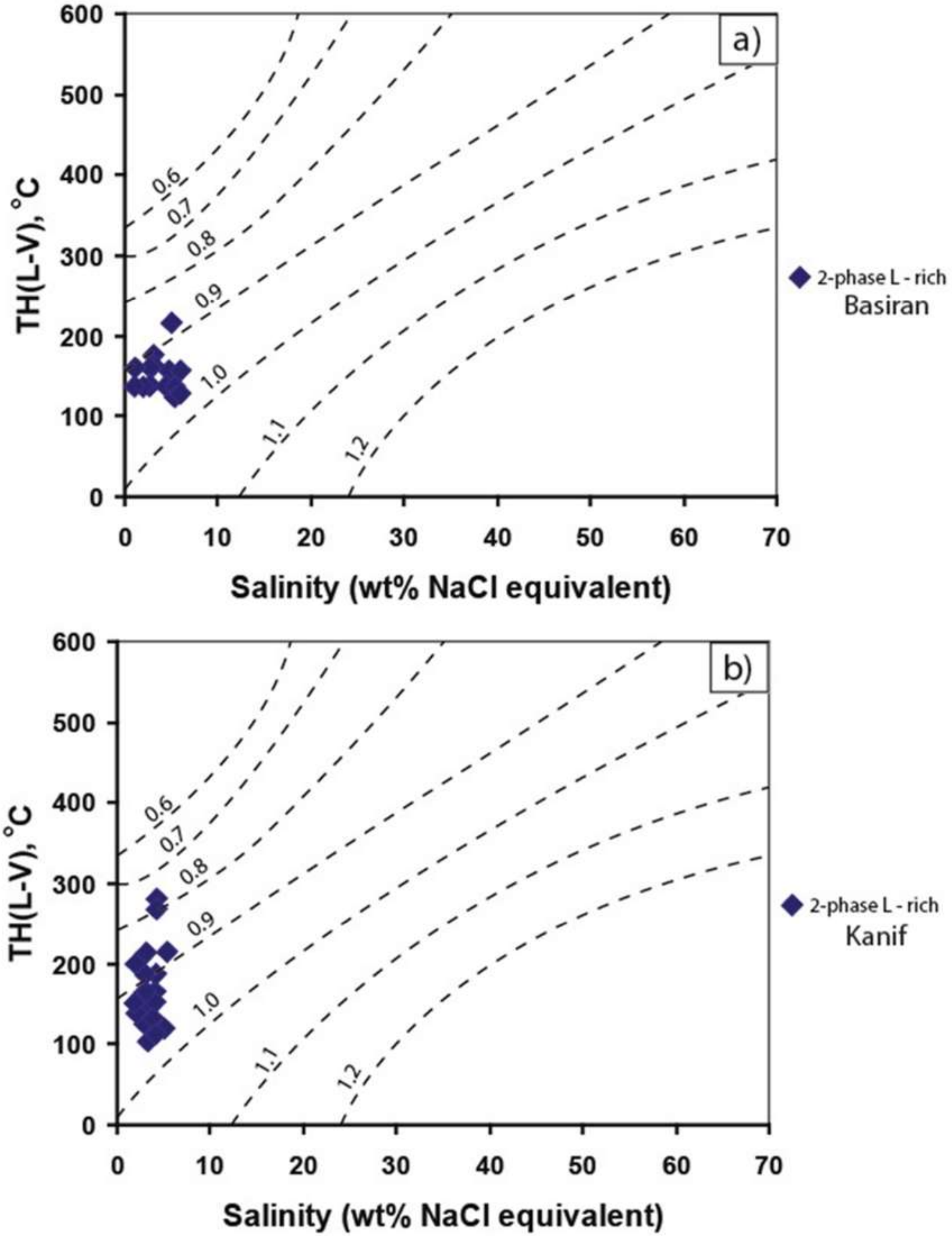

Fig.7 (a) plot of TH(L–V) versus salinity (expressed as wt% NaCl eq.) at Basiran. (b) plot of TH(L–V) versus salinity (expressed as wt% NaCl eq.) at Kanif. showing densities (in g/cm3) of the studied liquid-rich 2-phase fluid inclusions[1]. Contours regressed from data generated by the equation-of-state of Zhang and Frantz (1987)[8].

Table 1 Microthermometric data obtained from fluid inclusions within calcite crystals in the Mn ores at Basiran.

Sample	n	Size (μm)	Type	Tm (ice) °C	wt% NaCl	TH(L-V) °C
01	1	5	L+V	nv	.....	130

	2	5	L+V	nv	.....	140
	3	6	L+V	nv	.....	140
	4	10	L+V	-2.5	4.24	207
	5	7	L+V	-2.7	4.58	130
	6	5	L+V	-3	5.07	130
	7	7	L+V	-2.7	4.58	160
	8	10	L+V	-2.6	4.41	144
	9	9	L+V	-2.5	4.24	140
	10	7	L+V	-2.7	4.58	130
	11	7	L+V	-1.5	2.5	140
	12	7	L+V	-2.3	3.9	158
	13	6	L+V	-1.2	1.94	150
	14	7	L+V	-0.5	0.6	139
	15	5	L+V	-0.5	0.6	145
	16	10	L+V	-2.1	3.56	142
	17	5	L+V	-1	1.57	135
	18	7	L+V	-0.5	0.6	160
	19	8	L+V	-1.5	2.5	163
	20	10	L+V	-1.2	1.94	160
	21	10	L+V	-1.2	1.94	160
	22	10	L+V	-1	1.57	160
	23	10	L+V	-1.5	2.5	165
	24	8	L+V	-1.5	2.5	178
	25	5	L+V	-1.2	2.5	145
	26	5	L+V	-1.5	2.5	175

Table 2 Microthermometric data obtained from fluid inclusions within calcite crystals in the Mn ores at Kanif.

Sample	n	Size (μm)	Type	Tm (ice) °C	wt% NaCl	TH(L-V) °C
014-Br-56	1	8	L+V	-0.5	0.6	150
	2	8	L+V	-0.5	0.6	148
	3	7	L+V	-1.2	1.94	146
	4	10	L+V	-2.2	3.73	143
	5	10	L+V	-2.1	3.56	140
	6	8	L+V	-2.4	4.07	150
	7	7	L+V	-2.1	3.56	151
	8	22	L+V	-2.1	3.56	165
	9	1	L+V	-2.1	3.56	168
	10	8	L+V	-2.3	3.9	160

	11	1	L+V	-2.2	3.73	155
	12	6	L+V	-2.1	3.56	145
	13	7	L+V	-1.5	2.5	152
	14	7	L+V	-1.5	2.5	148
	15	7	L+V	-2.4	4.07	150
	16	8	L+V	-1.2	1.94	160
	17	5	L+V	-1.2	1.94	150
	18	7	L+V	-1.8	3.03	144
	19	7	L+V	-0.9	1.38	138
	20	7	L+V	-0.9	1.38	140
	21	8	L+V	-1.5	2.5	140
	22	12	L+V	-1.8	3.03	170
	23	8	L+V	-1.2	1.94	130
	24	9	L+V	-1.2	1.94	128
	25	10	L+V	-1.2	1.94	130
	26	8	L+V	-1.2	1.94	135
	27	18	L+V	-1.2	1.94	128
	28	12	L+V	-1.2	1.94	135
	29	10	L+V	-1.2	1.94	135
	30	5	L+V	-2	3.39	267
	31	6	L+V	-1.8	3.03	169
	32	10	L+V	-2.5	4.24	215
	33	10	L+V	-2	3.39	282
	34	8	L+V	-1	1.57	200
	35	8	L+V	-1	1.57	204
	36	5	L+V	-1.5	2.5	218
	37	8	L+V	-1.8	3.03	120
	38	15	L+V	-2.5	4.24	117
	39	10	L+V	-2.5	4.24	115
	40	10	L+V	-1	1.57	115
	41	6	L+V	-1	1.57	125
	42	6	L+V	-1.5	2.5	106
	43	10	L+V	-1.5	2.5	115
	44	10	L+V	nv	.....	114
014-Br-57	45	8	L+V	nv	.....	125
	46	5	L+V	nv	.....	129
	47	6	L+V	nv	.....	125
	48	7	L+V	nv	.....	115
	49	5	L+V	nv	.....	115
	50	5	L+V	nv	.....	125

	51	9	L+V	nv	.....	125
	52	7	L+V	nv	.....	130
	53	8	L+V	nv	.....	130
	54	5	L+V	nv	.....	100
	55	9	L+V	-1.6	2.68	125
	56	5	L+V	-0.6	0.80	130
	57	5	L+V	-1.5	2.5	100
	58	6	L+V	-1	1.57	155
	59	5	L+V	-1.5	2.5	125
	60	5	L+V	-1.7	2.86	125
	61	5	L+V	-1.7	2.86	120
	62	8	L+V	-1.4	2.31	135
	63	5	L+V	-1.4	2.31	117
	64	5	L+V	-1.5	2.5	185
	65	5	L+V	-1.5	2.5	115
	66	5	L+V	-1.6	2.68	145
	67	5	L+V	-1.5	2.5	135
	68	6	L+V	-1.5	2.5	118
	69	8	L+V	-1.5	2.5	155
	70	5	L+V	-1.7	2.86	160
	71	5	L+V	-1.4	2.31	125
	72	8	L+V	-1.3	2.13	196
	73	8	L+V	-0.7	0.99	180
	74	8	L+V	-0.7	0.99	178
	75	8	L+V	-0.7	0.99	150
	76	7	L+V	-0.9	1.38	150
	77	7	L+V	-0.7	0.99	206
	78	5	L+V	-1	1.57	195
	79	12	L+V	-1.7	2.86	190
	80	15	L+V	-1.3	2.13	190
	81	10	L+V	-1.6	2.68	185
	82	7	L+V	-1.7	2.86	180
	83	12	L+V	-1.7	2.86	190
	84	10	L+V	-1.7	2.86	185
	85	12	L+V	-1.3	2.13	189
	86	9	L+V	-1.3	2.13	185
	87	8	L+V	-0.7	0.99	175
	88	12	L+V	-0.7	0.99	180

References

1. Wilkinson, J.J. (2001) Fluid inclusions in hydrothermal ore deposits. Lithos 55, 229-272.
2. Shepherd, TJ, Rankin, AH, Alderton, DHM. (1985): A practical guid to fluid inclusion studies.Blackie Glasgow.
3. Aghanabati, A. (1998): Major sedimentary and stuctural units of Iran (map): Geosciences 7, 29-30.
4. Ahmad, S.N, Rose, A W. (1980): Fluid inclusions in porphyry and skarn ore at Santa Rita, New Mexico. Economic Geology 75, 229–250
5. Roedder, E. (1984): The Fluids in salt. Mineralogical Society of America Bulletin 69, 413-439.
6. Roedder, E. (1984): Fluid inclusions, Mineralogy Society of America Bulletin 12, 644p.
7. Bonatti, E., Zerbi, M., Kay, R., and Rydell, H. (1976) Metalliferous deposits from the Apennine ophiolites: Mesozoic equivalent of modern deposits from oceanic spreading center. Geol. Soc. Am. Bull., 87, 83-94.

Zhang, YG, Frantz, JD. (1987): Determination of the homogenization temperatures and densities of supercritical fluids in the system NaCl–KCl–CaCl2–H2O using synthetic fluid inclusions. Chemical Geology 64, 335–350.